The optical quantum-confined Stark effect and infrared-induced quenching in the emission spectra of quantum wells

2000 J. Phys.: Condens. Matter 12 5801

(http://iopscience.iop.org/0953-8984/12/26/325)

J. Phys.: Condens. Matter **12** (2000) 5801–5808. Printed in the UK PII: S0953-8984(00)12084-3

The optical quantum-confined Stark effect and infrared-induced quenching in the emission spectra of quantum wells

S M Sadeghi†‡§ and J Meyer‡

† Department of Physics, University of Toronto, 60 St George Street, Toronto, Ontario, Canada M5S 1A7

‡ The University of British Columbia, Department of Physics and Astronomy, 6224 Agricultural Road, Vancouver, B.C., Canada V6T 1Z1

E-mail: mostafa@physics.utoronto.ca (S M Sadeghi)

Received 24 February 2000, in final form 10 April 2000

Abstract. We study the optical quantum-confined Stark effect in the emission spectra of a symmetric quantum well coherently coupled by an infrared laser. It is shown that this effect is dynamically affected by the layer interface fluctuations and other defects, causing a field-dependent quenching of the emission spectra. We discuss how at low carrier densities the quenching process can be attributed to the intraband transitions between the populated exciton states and at high carrier densities to those between the conduction subbands.

Because of the device applications, a great amount of attention has been devoted to the study of the optical Stark effect in semiconductors [1]. In a bulk structure such as CdTe, this effect has been observed using a CO_2 laser to nearly resonantly couple the 1s and 2p states of the excitons [2]. The corresponding effect in quantum wells (QWs), the so-called optical quantum-confined Stark effect (QCSE), has also been investigated [3]. Here an intense CO_2 laser with polarization along the growth direction was used to couple the first (E1) and second (E2) conduction subbands. When E1 was detected from the valence band (figure 1(a)), the optical QCSE was observed in the absorption spectrum of the E1–HH1 excitons. Here, due to the excitonic nature of the intraband transitions, the coupling process can be more complex than those in bulk semiconductors or atoms. Depending on the QW structural parameters and the infrared laser frequency and intensity, these processes can be affected by the multi-subband or multi-state mixing of excitons. In the former case the laser mixes the exciton states associated with more than two conduction subbands [4]. In the latter case, however, the laser couples the 1s and 2s states of an exciton associated with a conduction subband with the 1s or 2s state of another exciton associated with a second subband, and vice versa [5].

In this paper we investigate the optical QCSE in the emission spectra of an infrared-coupled QW. To do this, in addition to the above-mentioned complexity, one should also consider the mechanisms responsible for the emission process. As discussed in references [6] and [7], depending on the sample temperature and the densities and energies of the photo-excited carriers, this process is not necessarily caused by the exciton population, but can be due

§ Author to whom any correspondence should be addressed.

0953-8984/00/265801+08$30.00

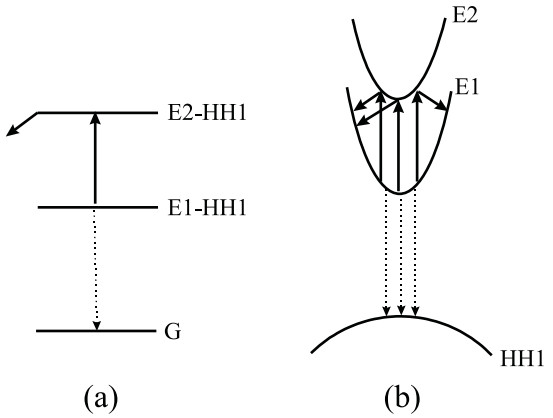

Figure 1. Schematic diagrams of the near-resonance infrared coupling of a QW when the PL emission is caused by the exciton population (a) or by the electron–hole radiative recombination at high carrier densities (b). The vertical thick arrows relate to the intersubband excitonic or electronic transitions caused by the CO_2 laser and the vertical dotted arrows represent the radiative transitions. The inclined arrows relate to the LO-phonon decay of excitons (a) or electrons (b).

to the contribution of the Coulomb correlation to the photon-assisted electron–hole radiative recombination. Therefore, to study the optical QCSE in the emission spectra of a QW we considered low carrier densities and low temperature where we could attribute the emission process to the population of the 1s states of the E1–HH1 excitons [7]. To avoid the complexity caused by the multi-subband and multi-state mixing processes, we considered a CO_2 laser near resonance with the transitions between the 1s states of the E1–HH1 and E2–HH1 excitons. By studying the emission spectra of the E1–HH1 excitons, we then investigated the effects of coherent coupling of these states and the roles played by non-radiative damping rates of excitons. Our results show that the emission spectra can undergo Stark blue- or red-shifts, to some extent, depending on the frequency of the CO_2 laser. In contrast to the optical QCSE in the absorption spectra of a QW [3], however, because of the dynamic effects of impurities, defects, and interface roughness, here these shifts are accompanied by an extensive amount of quenching. We explain various aspects of the quenching process and show how it is affected by the photo-excited carrier densities. This includes an investigation of the mechanisms responsible for this process in the limits where the emission spectra are caused by the exciton population and caused by the contribution of Coulomb correlation to the photon-assisted electron–hole radiative recombination.

For the exciton population limit, coherent effects in a system such as that shown in figure 1(a) can be described by the following parameters:

$$\gamma_{\mathrm{incoh}} = \frac{\Omega}{\Gamma_{\mathrm{E1-HH1}}} \tag{1}$$

$$\gamma_{\mathrm{coh}} = \frac{\Omega}{\Gamma_{\mathrm{E2-HH1}}}. \tag{2}$$

Here Ω is the Rabi frequency of the infrared laser coupling the E1–HH1 and E2–HH1 excitons, and $\Gamma_{\mathrm{E1-HH1}}$ and $\Gamma_{\mathrm{E2-HH1}}$ are the widths of these excitons. When $\gamma_{\mathrm{coh}} \ll \gamma_{\mathrm{incoh}}$, the coupling process mostly broadens the emission spectrum of the E1–HH1 excitons. For the intermediate case, $\gamma_{\mathrm{incoh}} \sim \gamma_{\mathrm{coh}}$, the spectrum broadens as it splits into a doublet. If $\gamma_{\mathrm{coh}} \gg \gamma_{\mathrm{incoh}}$, due to the quantum interferences a narrow dip or a dark line can be driven into the emission spectrum of the E1–HH1 excitons [8]. To examine these features in the emission spectra of a symmetric

QW, we used a hybrid CO_2 laser with $\sim$1 MW cm^{-2} intensity to couple the 1s states of the E1–HH1 and E2–HH1 excitons. This laser was p polarized; therefore its electric field had a component along the growth direction of the QW. The sample was grown by molecular-beam epitaxy (MBE) on a nominally undoped semi-insulating GaAs substrate. It contained fifty 7.3 nm undoped wells (GaAs) sandwiched between 18.1 nm barriers ($Al_{0.28}Ga_{0.72}As$). In order to pump the QW, a frequency-doubled Nd:YAG laser with 70 ps pulse width was used. This laser was focused at the surface of the QW within the area affected by the CO_2 laser. To justify using the exciton population limit, we reduced the sample temperature to 10 K and controlled the intensity of the Nd:YAG laser such that it generated $\sim 3 \times 10^9$ cm^{-2} carriers.

Figure 2(a) shows the results when the photon energies of the CO_2 laser were 121 meV, i.e. nearly 2.5 meV more than the transition energy between the 1s states of the E1–HH1 and E2–HH1 excitons ($\Delta \sim 2.5$ meV). One significant effect here is the strong quenching of the emission spectrum. This can be related to the fact that the E2–HH1 excitons decay very fast by emitting LO phonons. Therefore, as the CO_2 laser populates these excitons, they are disintegrated into electrons with relatively large wavevectors in E1 and holes at the bottom of HH1. Due to the presence of rough interfaces and other defects, this increases the chance of non-radiative recombination of these carriers before they form E1–HH1 excitons. Note that such a quenching process is different to those observed when, in addition to the pump laser responsible for generating excitons, the QW was exposed to an intense in-plane far-infrared laser [9] or to a visible laser [10]. In these cases no coherent intersubband transition between excitons occurs and the quenching occurred due to heating of electrons and holes or

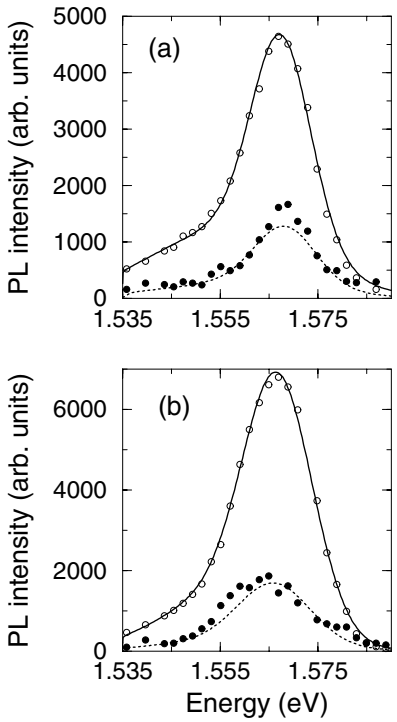

Figure 2. PL spectra of the QW in the absence (open circles) and presence (dots) of a CO_2 laser with $\sim$1 MW cm^{-2} intensity and (a) 121 and (b) 117 meV photon energies. The carrier densities are $\sim 3 \times 10^9$ cm^{-2}. The solid and dotted lines are the results from the theory.

ionizing E1–HH1 excitons [9], or via scattering of E1–HH1 excitons with photo-excited free carriers [10].

In addition to quenching, the spectrum in figure 2(a) shows some blue-shifting. This is a sign of the optical QCSE. Here, since the frequency of the laser was larger than the transition energy between 1s states of E1–HH1 and E2–HH1 excitons, the spectrum was blue-shifted. To see the optical QCSE when the frequency of the laser was less than this transition energy (negative detuning), we kept the carrier densities the same as those in figure 2(a) (3×10^9 cm^{-2}) but decreased the frequency of the CO_2 laser such that its photon energies became 116.5 meV ($\Delta \sim -2$ meV). Here, as figure 2(b) shows, we see a slight red-shift accompanied by a quenching similar to that seen in figure 2(a). When the CO_2 laser was less detuned ($\Delta \sim -1$ meV), the effect was a more drastic quenching of the emission spectrum (not shown).

To see the evolution of the quenching process with the carrier densities, we increased the intensity of the Nd:YAG laser. Figure 3 shows the differential emission intensity ($\Delta I/I$) when $\Delta \sim -2$ meV and the carrier densities were $\sim 10^{10}$ (empty squares) and $\sim 10^{11}$ cm^{-2} (filled triangles). The filled circles show $\Delta I/I$ for the data shown in figure 2(b), i.e. carrier densities of about 3×10^9 cm^{-2}. Figure 3 shows that the basic features of $\Delta I/I$ in the two limits where the emission spectra are caused by the exciton population (filled circles) and caused by the Coulomb contribution to the photon-assisted electron–hole recombination (filled triangles) are similar, to some extent. In each case, $\Delta I/I$ has two main features, A and B. The energies of features B and the amplitudes of features A are proportional to the carrier densities. In addition, the frequencies associated with the quenching minima, features A, are larger than those of the main emission peak in the absence of the infrared laser (vertical dotted line). This feature is an indication of red-shifting of the emission spectra. In addition, the slope of the quenching at frequencies larger than those of features A decreases as the carrier densities increase. This can be due to the phase filling of the high-energy states and the effects of the infrared coupling of

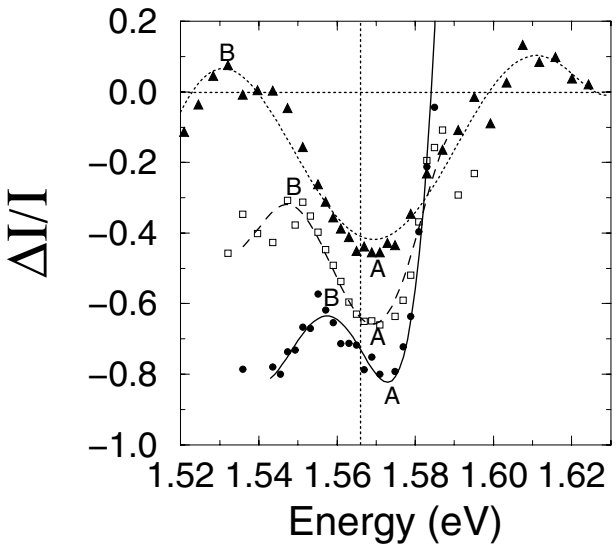

Figure 3. The differential PL emission intensity for various carrier densities. The filled circles relate to 3×10^9, empty squares to 10^{10}, and filled triangles to 10^{11} cm^{-2} carrier densities. The lines are to guide the eye. The vertical dotted line represents the approximate frequency of the emission peaks in the absence of the CO_2 laser.

the QW. Such a coupling process spreads electrons over a larger range of k-values compared to that in the absence of the CO_2 laser. This can increase the emission intensity in some regions, as seen in figure 3 for carrier densities around 10^{11} cm^{-2}.

To analyse the experimental results theoretically, we used the theory that we developed in reference [8]. Here, however, we included the effect of the non-radiative decay rate of excitons and estimated its value in the presence of the infrared coupling of E1–HH1 and E2–HH1 excitons. Briefly, within the rotating-wave and dipole approximations we consider the interaction of the laser with the QW using the following term:

$$H_1 = -\sum_{\boldsymbol{k}} \{\mu_{12} E(t) c^{\dagger}_{2,\boldsymbol{k}} c_{1,\boldsymbol{k}} + \mu^{*}_{12} E^{*}(t) c^{\dagger}_{1,\boldsymbol{k}} c_{2,\boldsymbol{k}}\}. \tag{3}$$

Here μ_{12} is the electric dipole matrix element for the transitions between the conduction subbands, which is assumed to be $\boldsymbol{k}$-independent, and $E(t) = E\mathrm{e}^{-\mathrm{i}\omega t}$ is the infrared field. $c_{i,\boldsymbol{k}}$ is the annihilation operator for an electron in the ith conduction subband with wavevector $\boldsymbol{k}$. Since the infrared laser mixes E1 and E2, in the presence of the pump (Nd:YAG laser), the electrons are distributed between these two subbands. Under the conditions of near-resonance coupling of E1 and E2 and low carrier excitation, the photo-excited electron–hole Coulomb interaction can then be given by the following:

$$V = \sum_{i\boldsymbol{k}\boldsymbol{k}'\boldsymbol{q}\neq\boldsymbol{0}} V_{\mathrm{HH1},i}(\boldsymbol{k}', \boldsymbol{q}) c^{\dagger}_{i,\boldsymbol{k}+\boldsymbol{q}} a^{\dagger}_{\mathrm{HH1},\boldsymbol{k}'-\boldsymbol{q}} a_{\mathrm{HH1},\boldsymbol{k}'} c_{i,\boldsymbol{k}}. \tag{4}$$

Here $a_{\mathrm{HH1},\boldsymbol{k}}$ refers to the annihilation operator for a hole in HH1 with wavevector $\boldsymbol{k}$.

Using equations (3) and (4) we calculated the equations of motion in k-space. These equations were then transferred to exciton bases. To do this we used the excitonic wavefunctions associated with HH1 and E1 and E2, $\phi^{n}_{\mathrm{HH1},i}$, obtained from

$$[E^{c}(i,k) + E^{h}(\mathrm{HH1},k)]\phi^{n}_{\mathrm{HH1},i}(\boldsymbol{k}) - \sum_{\boldsymbol{q}\neq\boldsymbol{0}} V_{i,\mathrm{HH1}}(q)\phi^{n}_{\mathrm{HH1},i}(\boldsymbol{k}+\boldsymbol{q}) = E^{i}_{n}\phi^{n}_{\mathrm{HH1},i}(\boldsymbol{k}). \tag{5}$$

Here E^{i}_{n} are the exciton binding energies associated with the ith conduction subband. The emission spectrum of the system was then obtained using linear response theory [8].

To apply this theory, note that the spectra in figure 2 are broad and have low-energy tails. These tails are caused by the localization of excitons in the potential fluctuations generated by the rough layer interfaces of the QW [11]. These fluctuations can also lead to large inhomogeneous broadening, making the PL spectra broad. The widths of the homogeneously broadened excitons (E1–HH1) contributing to these spectra are much less, however. At the temperature of our sample (10 K) the widths of the excitons that contributed to the low-energy tails (localized excitons) were $\sim$0.1 meV [12] and the widths of those that caused the main peaks (partially localized excitons) were $\sim$0.5 meV†. To include the effects of the inhomogeneous broadening, we convoluted the emission spectra of these excitons with two Gaussian envelope functions, one for the tail and one for the main peak. The functions considered were such that their sums fit the spectra in the absence of the IR field (figure 2, solid lines). We also considered the dephasing rate of E2–HH1 excitons ($\Gamma_{\mathrm{E2-HH1}}$) to be equal to 5 meV. This includes the fast scattering of the E2–HH1 excitons with LO phonons and the interface potential fluctuations.

The dotted lines in figure 2 are the results from the theory for the emission spectra in the presence of the CO_2 laser. They are obtained assuming the infrared-enhanced non-radiative decay rate of excitons to be equal to 0.3 ps^{-1}. This rate is associated with the transitions of electrons from the radiative 1s states of the E1–HH1 excitons to the non-radiative 1s states

† These are estimated on the basis of the particular specifications of our sample. In samples with narrower PL spectra the widths of the localized excitons are 0.1–0.2 meV (see reference [12]).

of the E2–HH1 excitons. It is also an indication of the strength of these transitions and how effectively electrons and holes are recombined non-radiatively after the E2–HH1 excitons are disintegrated by emitting LO phonons. As a result, the magnitude of this rate is related to the rate of scattering of these excitons with LO phonons and to the rough layer interfaces, impurities, and other defects in the sample. Note that the infrared-enhanced non-radiative decay rate of excitons does not play any role in the optical QCSE of the absorption spectrum of a QW. Therefore, in contrast to the emission case where quenching competes with the Stark shifts, in the case of absorption one can apply an intense infrared laser without significant quenching [3].

In addition to quenching, the strong broadening of the emission spectra in figure 2 also hindered observation of the optical QCSE. To see this in a semi-quantitative fashion and find out the roles played the intrinsic widths of the excitons, we consider the evolution of a homogeneously broadened exciton contributing to the peak of the emission spectrum in figure 2(a). The results in figure 4 show how the emission spectrum of such an exciton changes in the presence of a CO_2 laser with 1 MW cm^{-2} intensity and +2.5 (dashed line) or -2 meV (dotted line) detuning. Compared to that of the uncoupled spectrum (solid line), the amplitude of the emission spectrum has been reduced drastically—much more than those seen in figure 2. This is because in the homogeneously broadened case, in addition to quenching, we can also see the broadening caused by the coherent mixing of the E1–HH1 and E2–HH1 excitons. Such a broadening cannot be seen significantly in the inhomogeneously broadened spectra, since the contributions of the homogeneously broadened excitons overlap with each other.

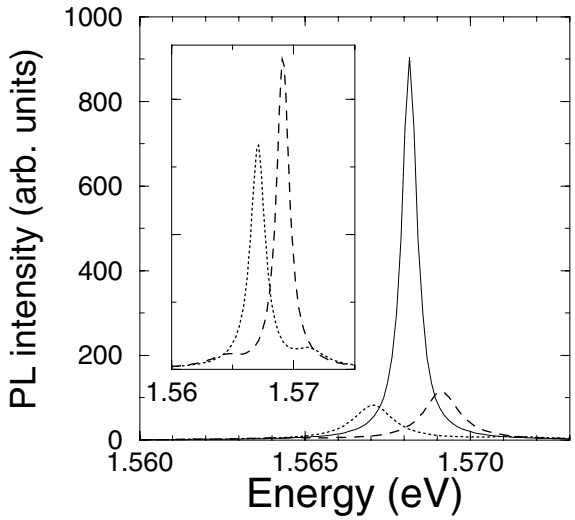

Figure 4. PL emission spectra of a homogeneously broadened exciton in the absence (solid line) and presence of a CO_2 laser with $\sim$1 MW cm^{-2} intensity and $\Delta = 2.5$ (dashed line) and $\Delta = 2$ meV (dotted line). The inset shows the details of the emission spectra in the presence of the CO_2 laser.

The dynamics seen in figures 2 and 4 are consistent with our expectation for the coherent processes in a QW system such as that shown in figure 1(a). Here, since $\Gamma_{\mathrm{E2-HH1}} = 5$ meV, based on equation (2) we have $\gamma_{\mathrm{coh}} = \Omega/5$. Also, since we considered $\Gamma_{\mathrm{E1-HH1}} = 0.5$ or 0.1 meV, depending on the energy of the excitons, $\gamma_{\mathrm{incoh}} = \Omega/0.5$ or $\Omega/0.1$. Under the assumption of $\mu_{12} \sim 2e$ nm, the Rabi frequency of the CO_2 laser is about 2.5 ps^{-1}. Therefore, since γ_{incoh} is large, we expect the dominant coupling process to be broadening of the emission spectrum (figure 4). On the other hand, although γ_{coh} is small, it is enough to cause small

features in tails of the spectra (see figure 4, inset). These features are the results of the coherences caused by the optical mixing of the E1–HH1 and E2–HH1 excitons.

The filled circles in figure 3 represent the values of $\Delta I/I$ associated with the results shown in figure 2(b). Since here the carrier densities are low, the features of $\Delta I/I$ can be explained in terms of the exciton population. As mentioned earlier, this involves infrared coupling of the populated exciton states, effects of localization and delocalization of the excitons, etc. At higher carrier densities these features remained similar, although the emission mechanism was different. Here, despite the presence of the Coulomb correlation, the radiative recombination process occurs when the electrons in E1 and the holes in HH1 have nearly the same wavevector magnitudes. On the other hand, since the effective masses of E1 and E2 for small wavevectors are similar and their energy spacings are close to that between the E1–HH1 and E2–HH1 excitons [13], the CO_2 laser can cause intersubband transitions between these subbands. Similarly to the case for the E2–HH1 excitons, the electrons in E2 emit LO phonons as they undergo intersubband transitions into E1 (figure 1(b)). Therefore, their wavevectors in E1 become very different to those of the holes, which are not affected by the infrared laser. As a result, some of the electron–hole pairs do not have the chance to recombine radiatively and the emission spectrum quenches. The similarities between the functions $\Delta I/I$ in figure 3 can therefore be related to the similarity between (i) the coupling process between E1 and E2 and (ii) that between E1–HH1 and E2–HH1.

Figure 3 also shows that as the carrier densities increase, the net amount of quenching decreases. This can partially be related to the carrier–carrier scattering processes. Here the incoherent contribution of these processes increases the dephasing rates associated with the E1–E2 transitions. This reduces the effect of the laser field, and causes a reduction in the quenching. This effect is particularly enhanced by the fact that in the presence of the CO_2 laser the distributions of electrons in E1 and E2 are no longer of Fermi–Dirac type [14]. In addition to this, at high carrier densities the transition energies are renormalized by various many-body effects and Coulomb interaction between electrons. This increases the CO_2 laser detuning, causing a reduction in the quenching.

In conclusion, we have studied the optical quantum-confined Stark effect and infrared-induced quenching in the emission spectra of a QW. The QW was coupled by a p-polarized CO_2 laser with photon energies close to that between the first and second conduction subbands. We showed that at low carrier densities the Stark blue- and red-shifts are accompanied by strong quenching caused by the intraband transitions between the excitons associated with the first and second conduction subbands. We also discussed how for near-resonance coupling the quenching mechanism remained unchanged for different levels of carrier density.

Acknowledgments

We are very grateful to T Tiedje and M Beaudoin for providing us with the sample. This research was supported by the Natural Sciences and Engineering Research Council of Canada.

References

[1] Krimer L O, Kalashnikov V L, Poloiko I G and Mikhailov V P 1999 *Opt. Spectrosc.* **87** 311
[2] Frohlich D, Uebbing B, Willms T and Zimmermann R 1994 *J. Lumin.* **58** 227
[3] Frohlich D, Wille R, Schlapp W and Weimann G 1987 *Phys. Rev. Lett.* **59** 1748
Frohlich D *et al* 1992 *Optics of Excitons in Confined Systems (Giardini Naxos) (Inst. Phys. Conf. Ser. 123)* ed A D'Andrea, R Del Sole, R Girlanda and A Quattropani (Bristol: Institute of Physics Publishing) p 227
[4] Sadeghi S M, Young J F and Meyer J 1997 *Phys. Rev.* B **56** R15 557
[5] Sadeghi S M, Meyer J, Tiedji T and Bedounin M 2000 to be published

[6] Kira M, Jahnke F and Koch S W 1998 *Phys. Rev. Lett.* **81** 3263
[7] Hagele D, Hubner J, Ruhle W W and Oestreich M 1999 *Physica* B **272** 328
[8] Sadeghi S M and Meyer J 1997 *J. Phys.: Condens. Matter* **9** 7685
[9] Quinlan S M, Nikroo A, Sherwin M S, Sundaram M and Gossard A C 1992 *Phys. Rev.* B **45** 9428
[10] Ashkinadze B M *et al* 1995 *Phys. Rev.* B **51** 1938
[11] Bastard G, Delalande C, Meynadier M H, Frijlink P M and Voos M 1984 *Phys. Rev.* B **29** 7042
[12] Jahn U *et al* 1996 *Phys. Rev.* B **54** 2733
[13] For experimental evidence see Vagos P, Boucaud P, Julien F H, Lourtioz J-M and Planel R 1993 *Phys. Rev. Lett.* **70** 1018
[14] Sadeghi S M, Leffler S R, Meyer J and Mueller E 1998 *J. Phys.: Condens. Matter* **10** 2489